BUILD SIMUL
https://doi.org/10.1007/s12273-023-0993-5

Design and optimization of thermally responsive autonomous dynamic glazed attachment systems for building solar heat gain control

Neda Ghaeili Ardabili, Yanxiao Feng, Julian Wang (✉)

Department of Architectural Engineering, Pennsylvania State University, University Park, PA 16802, USA

Abstract

Windows, as transparent intermediaries between the indoors and outdoors, have a significant impact on building energy consumption and indoor visual and thermal comfort. With the recent development of dynamic window structures, especially various attachment technologies, the thermal, visual, and energy performances of windows have been significantly improved. In this research, a new dynamic transparent louver structure sandwiched within conventional double-pane windows is proposed, designed, optimized, and examined in terms of energy savings in different climates. The uniqueness of the proposed design is that it autonomously responds to the seasonal needs prompted by solar heat gain through the use of thermally deflected bimetallic elements. Moreover, by integrating spectral selective louvers into the system design, the dynamic structure enables strong solar infrared modulation with a little visible variation. The optical and thermal properties of the dynamic glazing structure support about 30% and 16% seasonal variations in solar heat gains and visible transmittance, respectively. Furthermore, the potential energy savings were explored via parametric energy simulations, which showed significant potential for heating and cooling energy savings. This proposed design demonstrates a simple smart dynamic glazing structure driven by seasonal temperature differences, with significant solar heat control capabilities and minor effects on the visible or visual quality of the glazing system.

Keywords

smart window;
window attachment;
spectrally selective louver;
solar heat gain;
visible transmittance;
bimetal structure

Article History

Received: 30 November 2022
Revised: 13 January 2023
Accepted: 22 January 2023

© Tsinghua University Press 2023

1 Introduction

The significant amount of energy consumed by the building sector highlights the issue of sustainability in this industry. Some studies have focused on sustainability during construction (Syed et al. 2021), while others have explored sustainability during building operations (Chel and Kaushik 2018). Numerous publications have identified the building façade as a significant component of building operation, due to its substantial influence on energy consumption.

The significance of the façade in building energy consumption and occupant comfort has been studied in numerous publications, and techniques for improving overall façade performance have been offered (Sheikh and Asghar 2019; Bui et al. 2021; Rizi and Eltaweel 2021; Soudian and Berardi 2021; Barone et al. 2022; Le et al. 2022; Shafaghat and Keyvanfar 2022; Shen and Han 2022). The fundamental cause of the conventional façade's failure in terms of building energy performance and comfort is its constant nature, which does not accommodate variations in the outer environment. To that end, one proposed solution is the dynamic façade, which matches the façade's responsiveness to external circumstances and indoor demand (Wang et al. 2012). The mechanism of the dynamic façade is mainly defined by the problem it should solve.

Controlling solar heat gain while improving window thermal efficiency in response to diurnal and seasonal changes is what inspired this dynamic glazing system's design and development. As a result, the optimal scenario is one in which there is high solar heat gain during the heating-demand period and low solar heat gains during the cooling-demand period. Various glazing technologies such as chromic-based films, coatings, glazing systems

E-mail: Julian.wang@psu.edu

List of symbols

B	deflection of bimetal
E1	emissivity - front
E2	emissivity - back
EMS	energy management system
GHG	greenhouse gas
IGDB	International Glazing Database
L	length of bimetal
LSG	light to solar gain
Rsol1	solar reflectance - front
Rsol2	solar reflectance - back
Rvis1	visible reflectance - front
Rvis2	visible reflectance - back
SHGC	solar heat gain coefficient
t	thickness of bimetal
$T_{opening}$	transmittance passed through opening
Tsol	solar transmittance
Tvis	visible transmittance
α	transmittance factors through the strips attached to the deflecting frame during winter
α'	transmittance factors through the strips attached to the deflecting frame during summer
β	transmittance factors through the strips attached to the fixed frame

(Aburas et al. 2019; Aburas, et al. 2021; Kang, et al. 2022; Lei et al. 2022), automated dynamic shading systems (Al-Masrani and Al-Obaidi 2019; Wu and Zhang 2022), and automatic blind systems (Jung et al. 2019; Lin et al. 2020; Luo et al. 2020) were introduced to regulate solar heat gain. Chromic-based dynamic systems such as electrochromic and thermochromic dynamic glazings have been used in certain commercial buildings, but limited availability coupled with high product and installation costs have much curtailed the demand. Conversely, automated window attachments such as the shading and blind systems mentioned above are deemed the most cost-effective and have been widely adopted in both the commercial and residential sectors. As the design proposed in this work is more aligned with the technological pathway of ***automated window attachments***, to summarize their technical performance in terms of both solar heat gain control and visible transmittance, we have plotted the data for the most recent and presentative window attachment technologies in Figure 1.

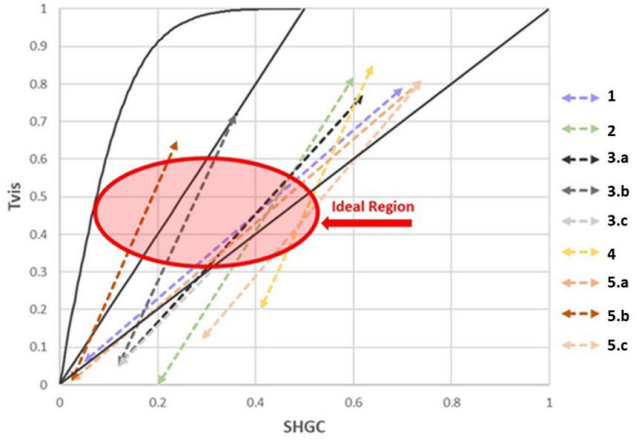

Fig. 1 Optical and thermal performances of window attachment technologies as presented in the studies 1 - (Montaser Koohsari and Heidari 2022), 2 - (de Vries et al. 2021), 3a, 3b, and 3c - (Atzeri et al. 2018)*, 4 - (Sun et al. 2021), 5a, 5b, and 5c - (Kunwar et al. 2019) (*Atzeri et al. (2018) did not directly report the SHGC, and the reported Tsol in the paper is converted to SHGC in the above graph)

As presented in the graph, there is a significant and positive correlation between the SHGC and Tvis of existing window attachment systems. As can be seen from Figure 1, most lines have high slopes, meaning that to achieve low SHGC properties, most attachment systems must eliminate nearly all visible light transmissions. As a result, the Tvis value is sacrificed to manage the SHGC. Conversely, some lines have relatively larger slopes, meaning that in systems where the Tvis value is the main objective of regulation, such large visible transmittance variations cannot help with controlling seasonal heat gain. In short, although great effort has been made to control the energy consumption and visual comfort of occupants by designing automated glazing attachment systems, their performance levels are limited to either overly narrow SHGC modulation capabilities or overly coupled SHGC and Tvis. In Figure 1, the ideal region is indicated based on previously reported performances in which the Tvis values were kept to a small change region, while the SHGC values had relatively more pronounced variations in different seasons. This is also considered as semi-uncoupled smart glazing systems, which have been demonstrated to deliver greater total energy savings across the U.S. climates compared to coupled or uncoupled Tvis and SHGC switching systems (DeForest et al. 2017).

Power use and associated operations are other concerns related to automated attachment-based dynamic glazing systems, including those discussed in the studies done by de Vries et al. (2021) and Sun et al. (2021). The systems discussed in Figure 1 suffered from increased installation complexities related to the actuation source (as compared to nonautomated systems). For these systems to have long-term

durability, attention should be devoted to designing for reparability, as minor actuator faults in the glazing or attachment power system should not create a requirement for major facade disassembly or reconstruction.

To address the above challenges, this study presents a new design with ***bimetal material-based transparent louver systems*** sandwiched in double-pane glass façades and illustrates its design process and solar heat gain control mechanisms. A computational design optimization was performed to address the spatial arrangement of multiple static and dynamic materials for a given optical behavior. More specifically, the dynamism of the design is triggered by seasonal outdoor temperature changes in order to regulate solar heat gains based on seasonal needs. A transparent louver system consisting of both static and dynamic sections is designed. Both sections of louver systems have spectral selectivity—high visible transmittance but low solar near-infrared transmittance. Actuating by the bimetal structures, the collective effects of both static and dynamic louver parts enable strong modulation in the solar infrared region (i.e., ~55% solar radiation (Duan et al. 2021)), while maintaining sufficient and stable photopic transmittance.

The remainder of this research is organized as follows. Section 2 discusses the process for the louver's structural design and optimization, an explanation of the intrinsic bimetal characteristic used in this design, the process for selecting the material for the middle layer, and the method for calculating the optical performance of the overall glazing system. Section 3 describes the dynamic system optimization findings, the optical performance of the material chosen for the design system, and the overall performance of the glazing system. Finally, Section 4 contains the final remarks.

2 Method

2.1 Problem definition and design workflow

The primary goal of this study was to maintain desirable visual transmittance while maximizing the solar heat gain variance between winter and summer (based on seasonal demands) for energy-saving purposes. The ideal case for winter is to transmit the full solar radiation, while the transmitted solar spectrum should be narrowed to the visible part for summer to control solar heat gain and retain small changes in visible transmittance.

In order to achieve this ideal case, this study proposes a dynamic louver system, where the deflection of bimetal supports the dynamism. The air gap between the two panes of the glazing system and the supported length of the bimetal that manages the deflection within the air gap restrictions serve as the design's primary limitations. Rhino_Grasshopper was the software used to design the transparent louver in this work. The design configuration was optimized with the Ladybug plugin for Grasshopper to obtain the maximum difference in the transmitted solar irradiance between summer and winter. Notably, the opaque louver systems were adopted at this optimization stage to simplify the design and optimization process. Subsequently, the appropriate spectral characteristics were identified from the International Glazing Database (IGDB) and applied to the louvers. To facilitate analysis in LBNL WINDOW, the designed layer was converted to a flat surface with the same optical properties; WINDOW's component - OPTICS was used for this conversion. Finally, to analyze the proposed system's performance, WINDOW was employed to simulate the optical and thermal performances and *EnergyPlus* was employed to simulate performance from an energy perspective. Notably, the major window modeling and simulation programs used in this work—*EnergyPlus* and LBNL WINDOW have been tested according to the standardized methodology, ANSI/ASHARE 140 and ISO15099, respectively, and both programs have been widely adopted and verified in other studies (Zhu et al. 2013; Curcija et al. 2015). The research flowchart is shown in Figure 2.

2.2 Bimetal material modeling and design

The thermal expansion coefficient difference between the two layers of bimetal causes thermally-triggered bending properties that allow the bimetal to be used widely across a variety of areas, such as temperature indication and control (Tcelykh et al. 2022) and function control (Furuto 2012; Li et al. 2020). In terms of function control, Li et al. (2020) proposed using a bimetal-driven shading system to control inlet solar radiation. Alternatively, in the Bloom Project, bimetal sheets were used as a responsive surface for controlling ventilation and shade (Furuto 2012).

In this study, the dynamism of the plane used to adjust the solar transmittance is accomplished through the automatic thermal-response feature of the bimetal. The dynamic louver is located between the two panes of the glazing system; consequently, a narrow gap (a typical double-pane window's gap width is 12 mm) between the panes restricts the design. The ends of the bimetal strips have fixed joints, so the movement of the dynamic glazed surface is supported by the beam-structured deflection of the bimetal. This study employed the two following equations (Eq. (1) and (Eq. (2)); the parameters are illustrated in Figure 3, alongside the two equations) to calculate the radii of the thermally deflected beam-structured bimetal strip.

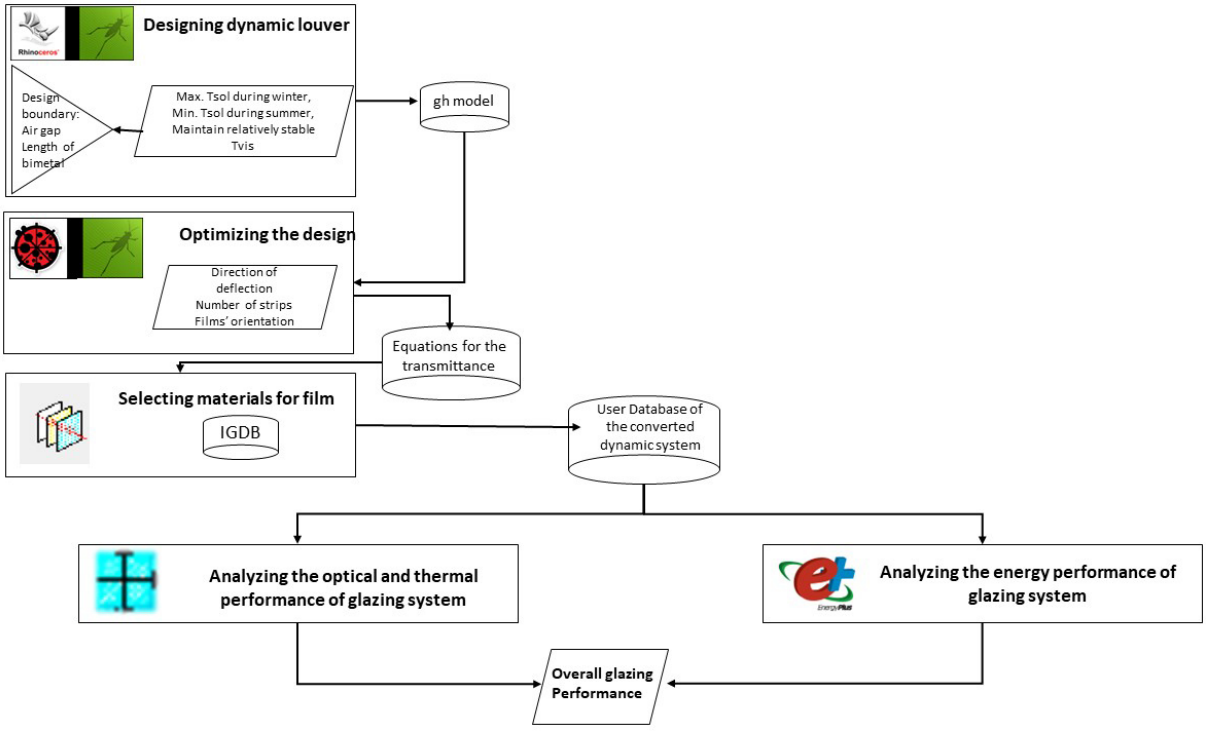

Fig. 2 Flowchart describing the design and optimization of the proposed system

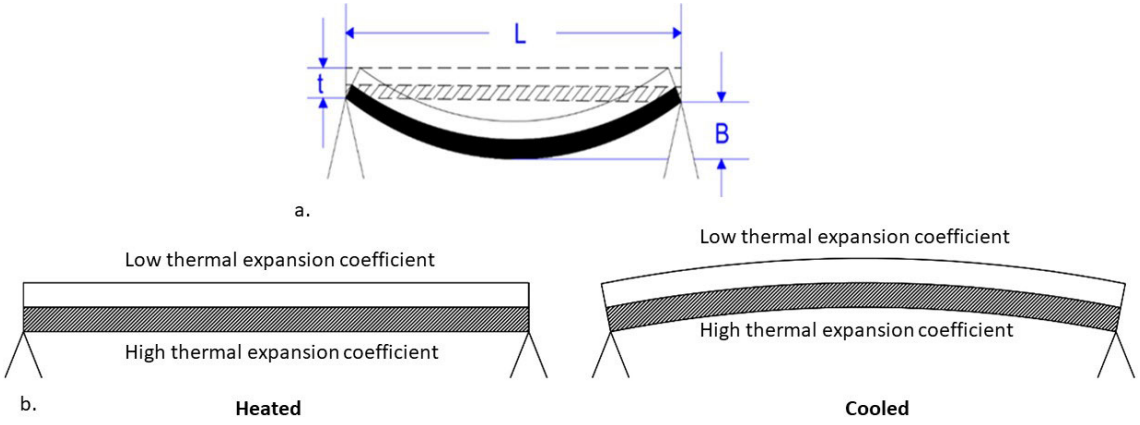

Fig. 3 (a) Beam-structured deflection of bimetal; (b) the reaction of the bimetal employed for the design in response to the temperature difference

$$\frac{1}{R} = \frac{8B}{L^2 + 4Bt + 4B^2} \tag{1}$$

$$\frac{1}{R} = \frac{\Delta T\left(\alpha_2 - \alpha_1\right)}{t} \tag{2}$$

Based on the above equations, the two variables B and t were kept at constant values of 12 mm and 0.13 mm, respectively. The 12 mm deflection was because of the maximum air gap in the double-pane glazing system, and the 0.13 mm thickness is the current minimum thickness of the bimetals. The variable ΔT refers to the bimetal material temperature difference between summer and winter, which drives the morphological change of the bimetal structure because of the different thermal expansion coefficients. In this work, this value was obtained based on the window's thermal transfer calculations in summer and winter conditions through LBNL WINDOW's THERM program. In particular, our initial calculation adopted the summer and winter conditions in Denver and double-pane windows, and the temperature difference in the air gap between summer and winter was 19.85 °C.

Based on these values, the approximate thermal expansion coefficient difference was calculated as 7.3×10^{-5}. To form such thermal expansion coefficient variations, a variety of bimetal materials could be used, such as antimony and potassium, cast iron, grey and potassium, and beryllium

copper and potassium. In this design, the bimetal strip was designed to be flattened at a high temperature but bent at a low temperature. Notably, one of the original motivations for this research was to leverage the existing, conventional, and even off-the-shelf bimetal materials and structures, facilitating potential scalability and manufacturing feasibility. Undoubtedly, some emerging thermally responsive materials such as two-way shape memory materials (Li et al. 2018) could be utilized to further increase the structural variations.

2.3 Dynamic structural design and optimization for the maximum winter-to-summer ratio

Rhino_Grasshopper was used for this design and optimization. Alternate strips of the film (referred to as deflecting strips) ends were perpendicularly attached to 10 cm bimetals. A series of these bimetals was then repeated to cover the window surface area. When the bimetals straightened, there was a flat striped surface; through their deflection, the strips were separated. Such variations altered the solar transmittance of the structure (see Figure 4). To simplify the optimization, the deflecting strips were assumed as opaque at this stage, and the optimization goal was to find out the greatest difference in transmitted solar irradiance in different seasons (i.e., summer and winter).

Galapagos Evolutionary Solver for Grasshopper was the generative design tool used to optimize this design. Galapagos is a genetic algorithm solver with machine learning principles that is used to find the optimum combination of the considered variables with fewer run sets (Zhang et al. 2020; Peres Suzano e Silva and Flora CaliliSuzano 2021). There are two reasons for selecting this tool for optimization. First, it is available on the Grasshopper platform and can easily be used with the parametric slider for the grasshopper model. Second, the Galapagos solver has been employed in other studies that have approved of the reported results. For instance, Abbasi Mahroo and Vafamehr (2022) optimized the Voronax roof structure via Galapagos to optimize the structure from a load-bearing perspective. Alternatively, researchers used Galapagos to optimize the predicted energy consumption (Ilbeigi et al. 2020). Lobaccaro et al. (2018) employed Galapagos to optimize the configuration to reduce GHG emissions.

"Genome" refers to the relationship between the variables used for optimization in the Galapagos Solver. The range of values for genomes in Grasshopper is limited to the slider parametric function. Three factors were offered for the genome to optimize in this study (see Figure 5):

a. Deflection direction: the indicator of the deflection direction of bimetals perpendicular to the windowpane; in this design, bimetals are deemed to be close to either the outer or inner pane of a double pane window; as a result, they may deflect toward the inside or outside, respectively. The considered deflection variable's genome slider range was 12 mm inward and outward. The deflection limit of 12 mm was chosen because this is the maximum gap for the present glazing system.
b. Orientation of the film strips between the two panes: it depicts the orientation of the film strips on the plane parallel to the window pane. At the time, the evaluated range for this variable was a 360-degree rotation at one-degree intervals.
c. Number of strips within the 10 cm bimetal: this variable determines the optimal number of strips that should be

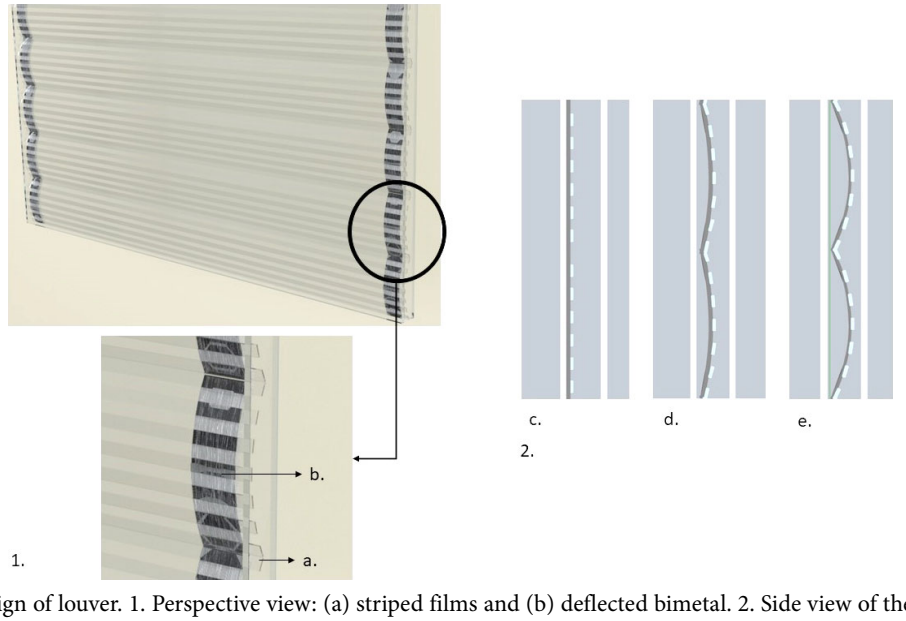

Fig. 4 Structural design of louver. 1. Perspective view: (a) striped films and (b) deflected bimetal. 2. Side view of the louver. In this view, two 10 cm bimetals are alongside: (c) flattened strips, (d) 6 mm deflected strips, and (e) 12 mm deflected strips

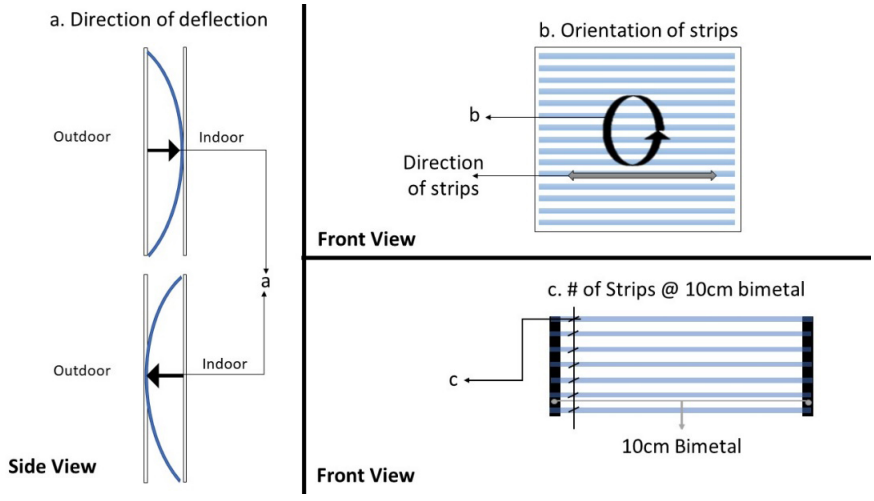

Fig. 5 Schematic definition of the considered variables for Genome

attached to the 10 cm bimetals; a range of three to twenty strips was employed for this variable. The thickness of the strips was utilized as the criteria for the number of strips within 10 cm. Because the thickness of the strips could be calculated by dividing 10 cm by the number of stripes and 20 pieces yielded 5 mm thickness for film strips, which was regarded as the minimum width of the strips from a practical standpoint, a maximum of 20 strips were evaluated.

Another important element in the optimization is the "Fitness Function" which is defined as the desired goal of the optimization and is accomplished by the relationship of parametric variables in the Galapagos Solver. The maximum ratio of the proportion of incident light during the winter to summer was the fitness of the solver. In total, 160 simulations were done to optimize the design parameters. In particular, the Ladybug plugin and the "IncidentRadaition" component were used to simulate incident solar radiation. A parallel surface with the window is defined within 25 mm of the window for computing incident radiation. Clear skies during the noon times in summer (July) and winter (December) in Denver were adopted in the design and optimization procedure. The seasonal proportions for both winter and summer were computed as the irradiation ratio on the parallel surface in the presence of the designed louver to the absence of it.

After optimization, the design was given one more layer: similar to the deflecting strips, alternate strips are attached to the fixed and flat frame (named fixed strips), and these strips are located in between gaps of deflecting strips to fill the earlier strips gaps (see Figure 6); as a result, from the front view, the whole system appears as a plane surface; while from the side view, the system is a series of strips that alternately have deflected and do not have deflected. Furthermore, if bimetals are flattened, and strips are spaced beside each other, this design creates a flat plane surface. This was done to ensure that the summer solar heat gain was as low as feasible and that the winter-to-summer radiation ratio was as high as possible. The optimized strip configuration for the hot season is a plane surface due to the flattened bimetal and positioned strips beside each other, and for the cold period, there is a maximum opening between the strips due to the deflected bimetal by 12 mm. This optimized system could achieve a winter-to-summer radiation ratio of 2.78.

2.4 Solar transmittance equations of the optimized louver system

The optimized louver configurations obtained above are based on opaque strips; however, our design goal is to maximize the winter-to-summer ratio while maintaining minor visible transmittance variations. The solar transmittance of the louver configuration can be mathematically expressed in the following generic equation (Eq. (3)). There are three ways by which solar incident on the dynamic louver system is transmitted inside: fixed strips, deflecting strips, and gaps between the fixed and deflecting stripes. As identified in Eq. (3), α, β, and T_{opening} are the portions of the total solar incidence transmitted through deflecting strips, fixed strips, and gaps between the strips, respectively. Furthermore, $T_{\text{deflected strips}}$ and $T_{\text{fixed strips}}$ are the solar transmittance of the deflected and fixed strips, respectively, which should be multiplied by their corresponding solar transmitted ratio.

The sum of the transmittance from fixed and deflecting strips, as well as the gaps between them, is regarded as the solar transmittance from the entire dynamic louver system without considering internal and external glass panes in this equation. Also, it should be noted that the fixed strips have a stable position, which inlets a fixed portion of the

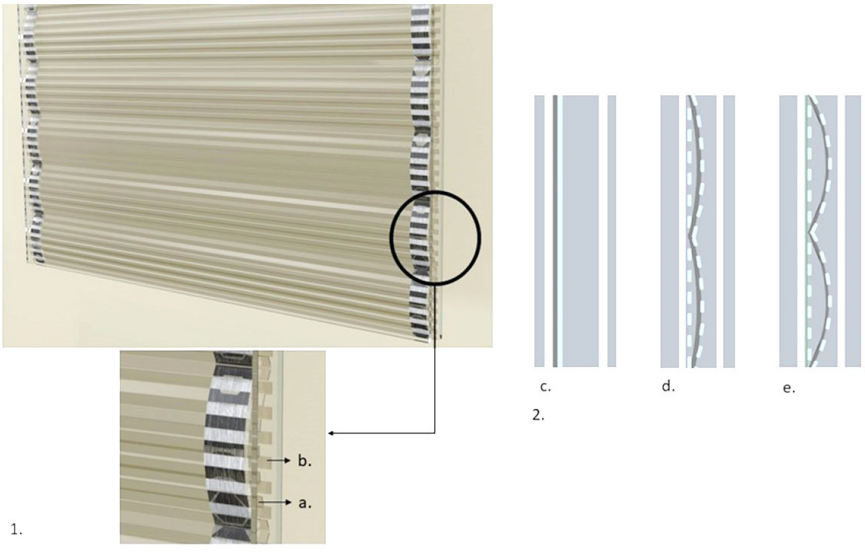

Fig. 6 Structural design of louver with new layer. 1. Perspective view: (a) strips attached to the deflected bimetal (deflecting strips) and (b) strips attached to the fixed frame (fixed strips). 2. Side view of the louver with a new layer. In this view, two 10 cm bimetals were alongside: (c) flatted strips, (d) 6 mm deflected strips, and (e) 12 mm deflected strips

incident solar radiation; therefore, the amount of β would be a constant value. However, the proportion inlet by deflecting strips and gaps between the strips vary by every millimeter of deflection; so, the factor α and T_{opening} vary by each millimeter deflection. For instance, when the bimetals are completely deflected, the factor T_{opening} is maximum; however, as the bimetals are flattened, the value of T_{opening} becomes zero since no portion of the incident light passes directly through the gaps in the system, and therefore section T_{opening} is eliminated from the equation for the summer situation as a result.

The winter-to-summer ratio of solar transmittance and the absolute difference between the winter and summer solar transmittance can be expressed as Eq. (4) and Eq. (5), respectively. Again, the transmittance factors should be kept low to achieve a high value for the absolute difference. It can be derived from these two equations that the solar transmittance for the deflected and fixed strips should be kept as low as possible, which guided us in identifying appropriate spectral or optical characteristics in next step.

$$T = \alpha T_{\text{deflected strips}} + \beta T_{\text{fixed strips}} + T_{\text{opening}} \tag{3}$$

$$T_{\text{winter}} / T_{\text{summer}} = \frac{\alpha T_{\text{deflected strips}} + \beta T_{\text{fixed strips}} + T_{\text{opening}}}{\alpha' T_{\text{deflected strips}} + \beta T_{\text{fixed strips}}} \tag{4}$$

$$\Delta = \left| (\alpha - \alpha') T_{\text{deflected strips}} + T_{\text{opening}} \right| \tag{5}$$

2.5 Multi-layer glazing system modeling and simulation

The WINDOW 7.8 library was used to extract the International Glazing Database and select a suitable film. As the solar transmittance should be low for the selected film, the factors of solar and visible transmittance were used during the selection. By following the strategy derived in Section 2.4., in the initial step, the threshold of solar transmittance below 0.1 was used to shorten the list; then, the filter of visible transmittance above 0.1 was employed to ensure that the selected materials were not dark surfaces blocking the view to the outside. Finally, the material with the highest Tvis and lowest Tsol was selected from the shortlist for both fixed and deflecting strips.

The optical properties of the films in every deflected situation were obtained using Eq. (3). The spectral data for the material was extracted using the OPTICS software, and the values of α, α', and β were calculated for every one-millimeter deflection. Supplementing the Tvis and Tsol values in Eq. (3) with the corresponding factors for deflection allowed for those variables to be calculated. The spectral data calculated as the user database in Text File format was imported into the OPTICS program to be saved in the library and imported to the LBNL WINDOW software to calculate the total glazing system properties.

WINDOW 7.8 was used to assess the properties of the entire glazing system. The triple glazing system, consisting of a central layer made of material rebuilt in OPTICS and two outer layers of clear glass, was chosen for the analysis. The distance between the two clear glasses was 12.6 mm, and the weighted mean was used to determine the middle layer's location, transforming the deflected layer into the flat one. While the converted middle flat layer was situated within 0.5 mm of the outer layer, the converted middle

layer with 12 mm deflection was inside the 4.2 mm outer layer. For every millimeter of deflection, the representative layer moved 0.3 mm toward the inner layer. The properties of the chosen clear glass are listed in Table 1 and Figure 7.

2.6 Energy performance simulation of the dynamic transparent louver system

The parametric energy simulation of the dynamic louver system was conducted via the Energy Management System (EMS) in *EnergyPlus*. Similar EMS-based parametric energy simulation methods have been adopted in other studies with dynamic parameters (Wang and Beltran 2016; Cedeno Laurent et al. 2017). The DOE ASHRAE 90.1 2019 prototype building model of a Large Office was selected for the simulation. In this comparative study, only building windows were changed. The baseline window properties are shown in Table 2; they complied with the most recent energy standards. Regarding the modeling of the dynamic window systems developed for this work, the setup components included: Sensor, Actuator, Program Calling Manager, Program, and Construction Index Variable. "Site Outdoor Air Drybulb Temperature" was chosen as the sensor for the program. The actuated components control type was "Construction State," and the selected items were the windows of the model. Program Calling Manager was set to "Begin Timestep Before Prediction." The program component was set by coding the "IF" statement, and the "While" loops and operation of the windows were defined according to the outdoor air temperature variation. Such parametric relationships were defined based on the glazing system analysis and derived regression functions in Section 3.3.1. Using the "Construction Index Variable" section, the optical and thermal properties of a representative glazing system, which was simulated using WINDOW LBNL software and defined in the "Window Material: Glazing" section of *EnergyPlus*, were labeled until the EMS recognized the defined construction, which would shift with the assigned temperature in the Program section. Unlike the optical and thermal optimization section, the proposed system was evaluated for all eight ASHRAE climate zones: Honolulu, HI, Tampa, FL, Atlanta, GA, Seattle, WA, Denver, CO, Rochester, MN, International Falls, MN, and Fairbanks, AK and referenced as Climate Zones 1 to 8, respectively. The reason for selecting these climate zones was the availability of the weather data of the location in EPW format to simulate the *EnergyPlus*.

For the simulation, instead of defining the different "While" loops for the various glazing constructions generated in LBNL WINDOW for every deflection interval, two glazing constructions in which the dynamic louver system was totally deflected and flat were considered; the switch point between these two constructions was the mean of the reported Monthly Design Dry Bulb temperature for the coldest and hottest months listed in ASHRAE Climatic Design Conditions 2021 (see Figure 8). Two reasons support this method for deciding the switch temperature. First, our previous study explored (Hinkle et al. 2022) the impact of the threshold temperature on the optimum performance of the proposed structure. Four temperatures were considered for evaluation, and 10 °C, which is approximately the middle of the hottest and coldest design temperatures for Denver,

Table 1 Optical properties of the clear outer glass in the glazing system

ID	Name	Thickness (mm)	Tsol	Rsol1	Rsol2	Tvis	Rvis1	Rvis2	E1	E2
22501	0.5t_ATG.GLW	0.5	0.919	0.077	0.077	0.92	0.079	0.079	0.84	0.84

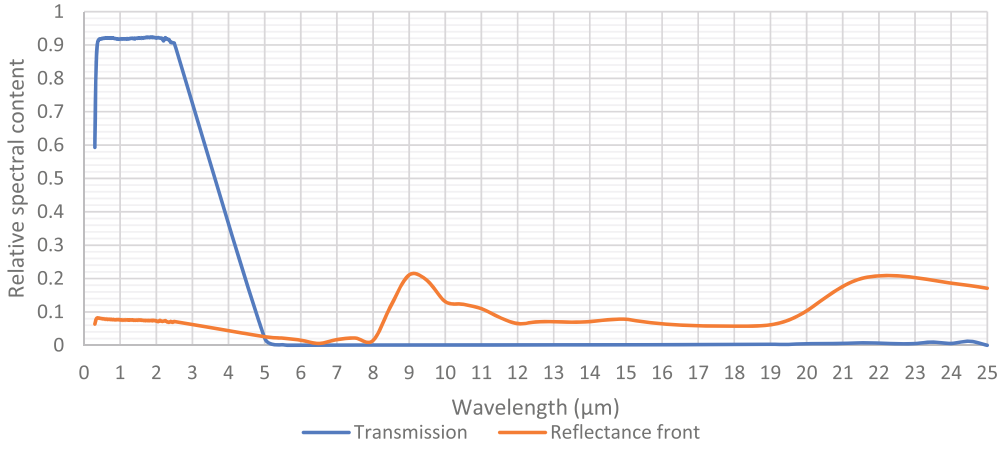

Fig. 7 Spectral curve of the clear glass chosen for the outer panes of the glazing system

Table 2 Thermal and optical properties of the windows of the base model

Climate zone	U-factor	SHGC	Tvis
Z1	2.84	0.23	0.253
Z2	2.61	0.25	0.275
Z3	2.38	0.25	0.275
Z4	2.04	0.36	0.396
Z5	2.04	0.38	0.418
Z6	1.93	0.38	0.418
Z7	1.65	0.4	0.44
Z8	1.48	0.4	0.44

Table 3 Switch point temperatures for the glazing system in EnergyPlus simulation

Climate zone	Switch point (°C)
Z1_ Honolulu, HI	25.5
Z2_ Tampa, FL	22.3
Z3_ Atlanta, GA	16.8
Z4_ Seattle, WA	12.2
Z5_ Denver, CO	11.7
Z6_Rochester, MN	6.05
Z7_Internatioanl Falls, MN	1.95
Z8_ Fairbanks, AK	−2.6

CO, showed the optimum performance for that system with regards to saving energy. Second, in the present research, the simulation of Climate Zone Five _Denver, CO was used for both methods of several loops for every millimeter deflection and two loops for the completely deflected and flat situations. The results were very close to one another. The heating load for the two setpoints was 2.25% less than for the case with 12 setpoints, while the cooling load was 0.008% less than for the case with 12 setpoints and the "While" loops. Consequently, for ease of simulation, the two dynamic window states were considered for the "While" loop. The temperatures considered as the switch points, the average of the hottest and coldest design temperatures for the seven climate zones, are listed in Table 3.

3 Results and discussion

3.1 Optimal transparent louver system design

According to the optimization results, seven 7.7 mm wide strips of the film should be alternately joined to the 10 cm bimetal. Six strips of film of the same width should be alternatively fastened to the fixed frame to cover the gaps between the seven strips on the bimetal. Because the orientation of the strips is 90 degrees in the optimization output, the strips should be vertical. In terms of deflection, the ideal scenario is attained when the strips are deflected 12 mm inward in the winter and flat, with no deflection, in the summer. Thus, the strips should be placed near the outer glass to allow for deflection. Figure 9 depicts the optimal location of the strips at solar noon in the summer and winter seasons, respectively. As depicted in Figure 9, the series of the 10 cm bimetal with the supplementary fixed frames are repeated aside the window to cover the entire window surface. It should be noted that both frames_bimetal and fixed_are embedded inside the window frame, and in Figure 9, they are depicted outside the window frame to illustrate the dynamic louver structure explicitly. As for the dynamism of the system, according to the results of the direction of deflection optimization, the system will be flat at high temperatures, and it will start to deflect and provide the opening between the strips as the temperature decreases.

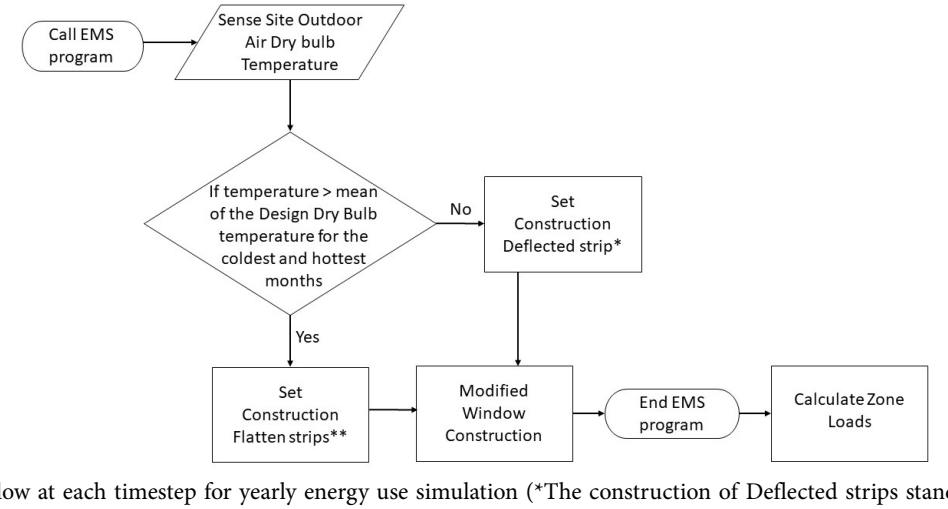

Fig. 8 EMS workflow at each timestep for yearly energy use simulation (*The construction of Deflected strips stands for the situation where the dynamic louver system has completely deflected and provides the maximum opening. **The construction of Flatten strips stands for the situation the dynamic louver system has completely flattened, and there is no opening in the system)

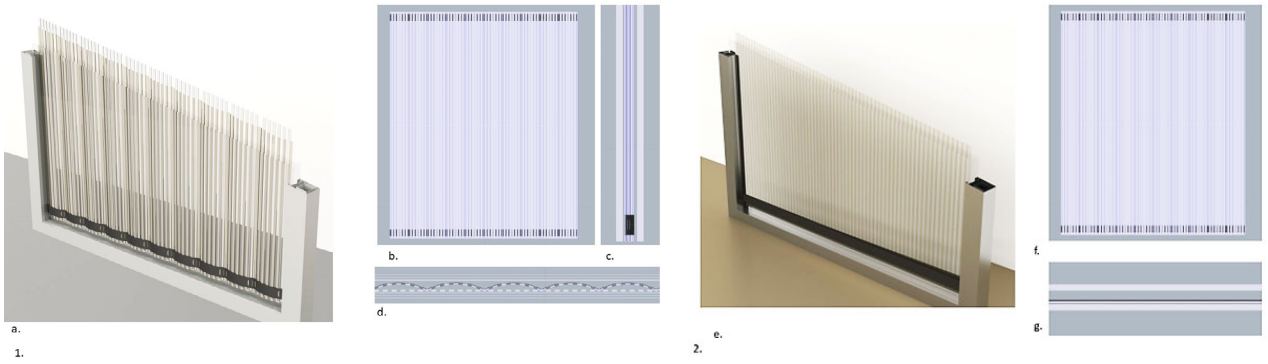

Fig. 9 Optimal louver structure. 1. Louver with 12 mm deflection; beige strips represent the deflecting and fixed strips, respectively: (a) perspective view, (b) front view, (c) side view, and (d) top view. 2. Louver with no deflection; beige strips represent the deflecting and fixed strips, respectively: (e) perspective view, (f) front view, and (g) top view

Factors affecting the solar transmittance in Eq. (3) for the optimum situations in summer and winter were calculated based on the simulation in Ladybug Grasshopper. The variable α was used to represent the transmittance factor through the deflecting strips. These factors varied according to the deflection of the bimetals. For example, in winter, when there is maximum deflection, the incident radiation on the vertical surface beneath the louver was 0.7. As a result, while 0.7 of light was transmitted through the gaps caused by the deflection, 0.3 was the portion that struck the deflecting strips. The amount of its transmittance relied on the film's transmission. Based on the same logic, the value of β could be calculated, and since this factor belonged to the fixed strips, in all situations, the value of β was a constant value of 0.46. The value of the opening was related to the amount of transmission through the gaps caused only by the deflection. Table 4 lists the values of the factors in Eq. (3) related to deflection.

Table 4 Factors calculated for α and β

Deflection (mm)	$T_{opening}$	α	β
12	0.274	0.3	0.46
11.5	0.251	0.34	0.46
11	0.198	0.4	0.46
10.5	0.149	0.46	0.46
10	0.090	0.53	0.46
9	0.081	0.54	0.46
8	0.073	0.54	0.46
7	0.065	0.54	0.46
6	0.057	0.54	0.46
5	0.047	0.54	0.46
4	0.039	0.54	0.46
3	0.032	0.54	0.46
2	0.021	0.54	0.46
1	0.009	0.54	0.46
0	0.000	0.54	0.46

Based on Table 4 factors calculated for Eq. (3), the solar transmittance for summer and winter design conditions were determined as follows (Eq. (6), Eq. (7)):

$$T_{winter} = 0.3T_{deflected\ strips} + 0.46T_{fixed\ strips} + 0.274 \quad (6)$$

$$T_{summer} = 0.54T_{deflected\ strips} + 0.46T_{fixed\ strips} \quad (7)$$

Based on the estimated equations for transmittance for the winter and summer, the solar transmission of the chosen film should be low to keep the ratio T_{winter}/T_{summer} (Eq. (4)) as high as feasible. Similarly, to attain a considerable value for the absolute difference Δ, the solar transmittance value should also be kept low. Accordingly, a relatively lower solar transmittance should be pursued when choosing the film for this dynamic glazing design.

3.2 Solar optical behaviors of the louver attachment system

The selected material for both fixed and deflecting strips was coated glass with an ID of 18517 at IGDB. Its thickness was modified to 1.6 mm in OPTICS 6.0. Table 5 and Figure 10 list the properties of materials at a 1.6 mm thickness.

The Tvis and Tsol values from the spectral data of the selected materials were input into Eq. (3) to generate the converted layer for every deflection interval in OPTICS and saved as new materials in the library. Figure 11 shows the spectral curves for all converted layers.

According to Figure 11, as the deflection increased, so did the transmittance; however, while the increment trends of the Tsol values between the flat and 9 mm deflections were the same, the increment trend for the Tsol values between the 10 mm and 12 mm deflections had higher intervals; thus, for a more accurate analysis, the interval level between the 10 mm and 12 mm deflections was decreased to 0.5 mm.

In this work, the temperature gradient from summer to

Table 5 Optical properties of the selected materials

File name	Thickness (mm)	Solar, T	Solar, Rf	Solar, Rb	Photopic, T	Photopic, Rf	Photopic, Rb	Emit, F	Emit, B
6 Low-E N 31_18_ATL.TEG	1.6	0.134	0.254	0.57	0.332	0.189	0.138	0.84	0.031

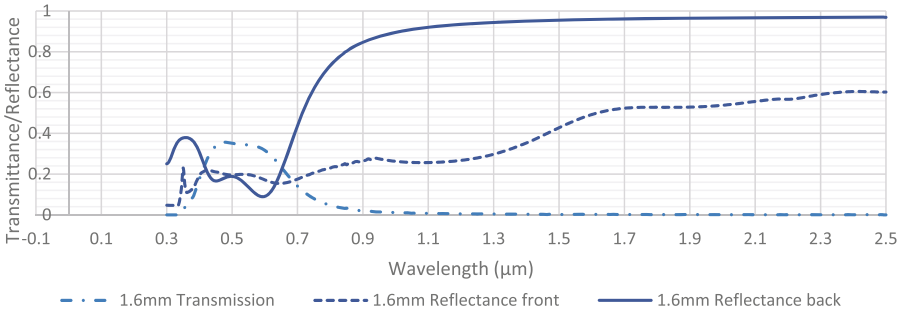

Fig. 10 Spectral transmittance and reflectance curves of the selected materials with a thickness of 1.6 mm

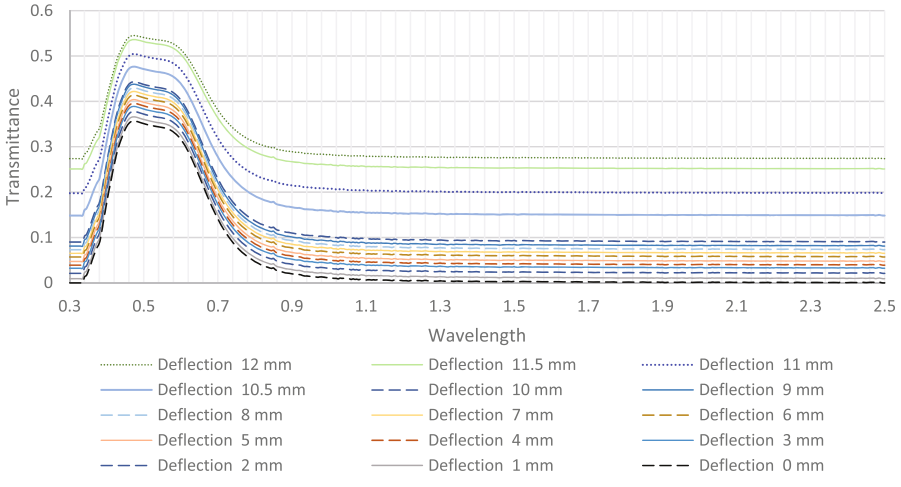

Fig. 11 Spectral transmittance curves of the converted layers in OPTICS

winter was used as the actuator for the variations in the bimetals' deflection. The selected bimetal should be deflected at the cold temperature and then flatten with an increase in temperature to provide a flat surface in the summer season. In this research, the average design temperature for June, July, and August was indicated as the summer temperature, and for winter, the mean design temperature during December, January, and February was considered. The mean design temperature for winter was 0.53 °C and the mean temperature for summer was 20.38 °C. As a result, the bimetal should be deflected to 12 mm with a 19.85 °C variation between the summer and winter seasons. The required temperature drops and corresponding Tvis and Tsol values for every deflection interval are listed in Table 6.

Table 6 only presents the Tsol and Tvis values for the middle layer, and these will be changed by incorporating other layer information into the double-pane glazing system. Still, note that the proposed design achieved a significant modulation of solar transmittance while maintaining a

Table 6 Temperature drops calculated for every deflection interval and the corresponding optical properties

Deflection	Design temperature	Tsol	Tvis
12	0.53	0.372	0.523
11.5	1.27	0.358	0.517
11	2.02	0.313	0.484
10.5	2.78	0.272	0.455
10	3.56	0.223	0.419
9	5.13	0.215	0.413
8	6.73	0.207	0.405
7	8.37	0.199	0.397
6	10.03	0.191	0.389
5	11.71	0.181	0.379
4	13.42	0.173	0.371
3	15.15	0.166	0.364
2	16.88	0.155	0.353
1	18.63	0.143	0.341
0	20.38	0.134	0.332

desirable visible transmittance. The solar transmittance could be adjusted from 0.134 to 0.348, leading to an almost three-fold difference, while the visible transmittance saw a much smaller change, from 0.332 to 0.457. This demonstrates that the designed structure and selected material worked properly and could be used to control solar heat gains in different seasons with only small variations in Tvis, conclusions that align with the original expectations for this research.

3.3 Overall performance of the glazed façade

In this section, the overall double-pane glazing system was constructed with the above-described design, and the bimetal louver system was analyzed via the WINDOW modeling and simulation program.

3.3.1 Thermal and optical performance

Fifteen layers converted into OPTICS were imported into LBNL WINDOW to obtain the overall performance of the louver in the glazing system. Table 7 and Figure 12 present the glazing system's overall performance. Notably, the information in Table 7 was for the overall glazing system, while Table 6 only displayed the original central layer's optical performance. Moreover, taking both Tvis and SHGC into account, the light-to-solar-gain (LSG) ratio was introduced and added to this table. LSG indicates how well a glazing system controls visible light and infrared thermal radiation. Because the central transparent louver system is ultra-thin and not made from insulating materials, it did not add noticeable changes to the typical double-pane windows due to the louver behaviors.

Table 7 Properties of the double-pane glazing with the designed louver system

Deflection	Temperature	SHGC	Tvis	LSG
12	0.53	0.455	0.452	0.993
11.5	1.27	0.441	0.448	1.016
11	2.02	0.401	0.420	1.047
10.5	2.78	0.362	0.395	1.091
10	3.56	0.311	0.365	1.173
9	5.13	0.300	0.360	1.200
8	6.73	0.288	0.353	1.225
7	8.37	0.277	0.346	1.249
6	10.03	0.265	0.339	1.279
5	11.71	0.251	0.330	1.315
4	13.42	0.238	0.323	1.357
3	15.15	0.224	0.317	1.415
2	16.88	0.205	0.307	1.498
1	18.63	0.181	0.297	1.641
0	20.38	0.156	0.289	1.853

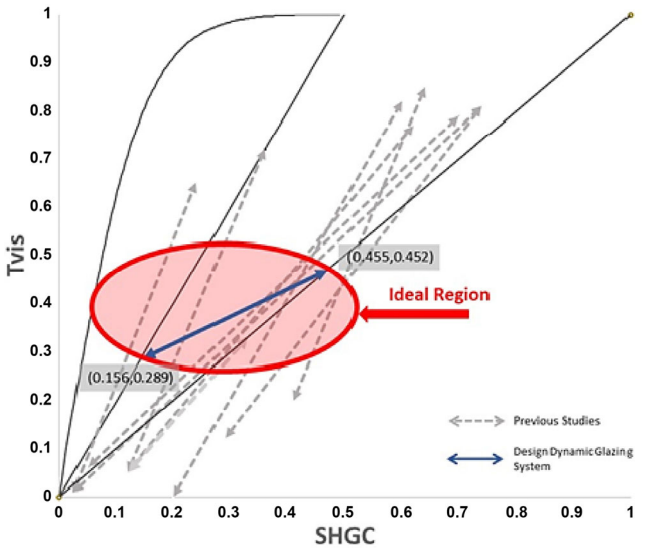

Fig. 12 Tvis-to-SHGC ratio for the louver system at each deflection interval

As presented in Table 7, the SHGC moved from 0.156 to 0.455 with total deflection of the louver system, meaning about a 30% solar heat gain variation in different seasons; the variation in Tvis of the glazing system with total deflection of the louver system was 0.289 to 0.452, equal to about a 16% seasonal variation. After plotting the changes in Tvis and SHGC in the baseline-technology diagram (see Figure 1), Figure 12 shows that the designed system fell within the pre-defined ideal region. Although certain linear relationships still existed in this design, as expected, this designed system had a much better performance in modulating SHGC while maintaining a smaller variation in Tvis (i.e., the relatively lower slope of the line). Regarding the LSG variations, in general, under stable visible transmittance situations, a high LSG value manifests in the glazing transmitting less solar heat gain, which is most effective in the summer season, while a low LSG value indicates relatively more solar heat gain, referring to the energy savings benefits in the winter season (Wang et al. 2016). This also aligns with the LSG variations seen with the present design. Table 7 shows that during the winter, with the complete deflection of the strips, the LSG value was close to 1, indicating that the glazing system transmitted the same fraction of solar heat as solar light. However, by decreasing deflection and converting the louver system to a flat surface during the summer, the LSG became 1.85, meaning that the amount of transmitted light was 1.85 more than the solar heat.

Furthermore, two regression relationships, SHGC vs. temperature and Tvis vs. temperature, were able to be derived and are presented in Figure 13. Obtaining these two relationships will enable whole-building energy simulations to incorporate such dynamic glazing characteristics.

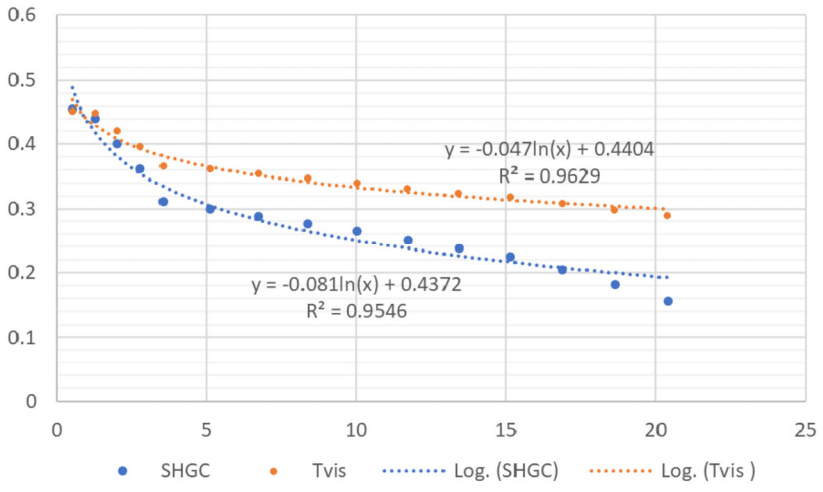

Fig. 13 Correlation between the temperature and glazing system's SHGC and Tvis

3.3.2 *Energy performance simulation and analysis*

Annual heating, cooling, and lighting loads were analyzed in eight cities representative of eight climate zone in the US. The simulated model was the DOE prototype building for a large office and incorporated the dynamic louver glazing system into the model's windows. Figure 14 illustrates the details of heating and cooling energy use in the model with the dynamic system compared to the basic model. In addition, the same comparison was made for lighting energy use and the results are reported in Figure 15. The energy use was also reported separately in Figure 16 to provide a more in-depth picture of the glazing system's energy performance.

As depicted in Figure 14 and Figure 16, the dynamic system performed differently in the various climate zones. In general, the dynamic system was most effective for areas where the heating and cooling loads were equivalently high (Zones 4 and 5), or the heating load was slightly more than the cooling load (Zones 6 and 7), and the energy savings ranged from 15% to 30%. Comparatively, by increasing the cooling demand in the model (as in Zones 1 and 2), the dynamic system's implementation became ineffective and burdened the model with an extra load. This seems different from the prior dynamic glazing studies, which are mainly effective in hot climates. This can be explained by the specific dynamic SHGC range (0.156–0.455) obtained in this design, which is relatively more beneficial to the winter seasons, reducing heating loads. Notably, with the established analytical functions (Eqs. (3), (4), and (5)), the solar transmittance of the strips and/or window panes can be simply adjusted to bring the dynamic SHGC range to low levels (e.g., 0.05–0.2), which may be more beneficial to hot climates. From the

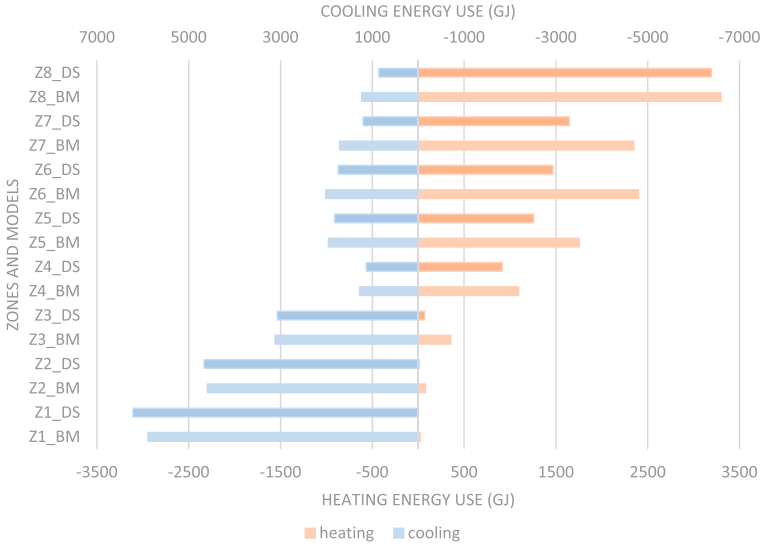

Fig. 14 Annual heating and cooling energy use comparison (BM stands for Base Model, and DS stands for the model with dynamic systems)

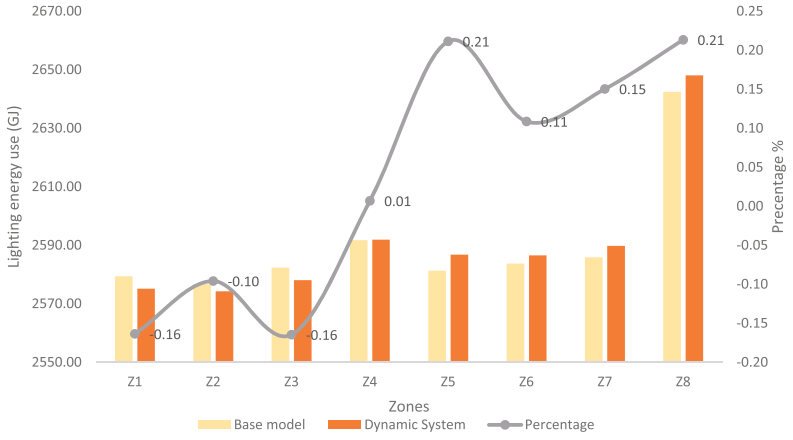

Fig. 15 Annual lighting energy use comparison

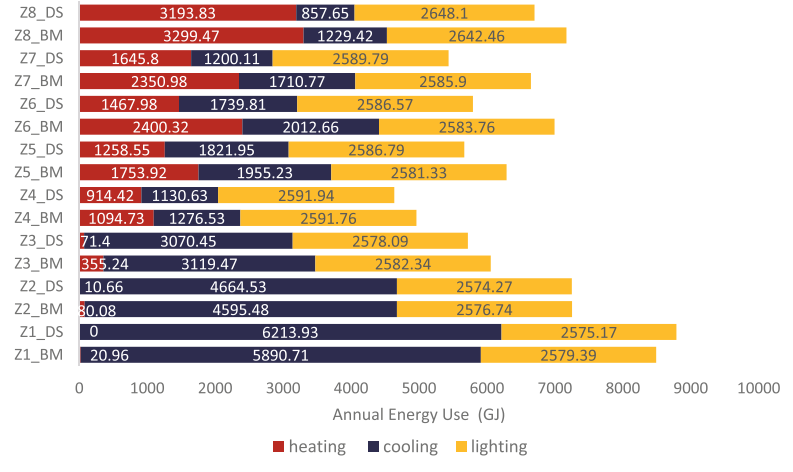

Fig. 16 Comparison of the annual heating, cooling, and lighting energy consumption levels

lighting energy side, as presented in Figure 15, there was a minor difference between the implementation of the dynamic system and the baseline model, which is mainly due to the differences in the Tvis values between the designed system and the baseline models. As mentioned in the Introduction section and shown in Figure 1, most dynamic attachment systems have to compensate for electrical lighting energy to achieve lower SHGC values, which is an important issue for summer seasons or hot climates. Comparatively, Figure 15 presents that the designed dynamic system in this work didn't significantly affect electrical lighting energy as the system maintained relatively stable and desirable Tvis when modulating SHGC.

Additionally, the purpose of the energy impact analysis in this work was to verify the potential benefits of the designed system rather than deeply searching or computing the optimal settings of the designed system for each different climatic zone. As such, the results here are based on a simple selection of the transition temperature based on the maximum and minimum design temperatures and the same dynamic SHGC range across all climates. To suit different climatic conditions and building characteristics, certain optimization works are needed, in terms of transition temperature settings, initial and ending temperature points for deflection, and more importantly, the solar optical properties of the strips. This will be considered for our future research.

4 Conclusion

The current study designed, optimized, and examined a new dynamic transparent louver attachment system implemented between conventional double-pane windows. By embedding thermally responsive bimetallic elements, the deflection of the central transparent louver structures could produce significant modulations in solar transmittance (~30%) while maintaining much less change in visible transmittance (~16%). The results realized a substantial fluctuation in SHGC and a minor difference in Tvis, which aligns with the expected semi-uncoupled control of solar light and heat

for building glazing systems. This also makes the suggested structure ideal for climates where both heating and cooling are required, and the variation in SHGC matched the seasonal demands at virtually constant visible light transmittance. The present study presents the details of this design process from structural design/optimization to spectral characteristics determination and multilayer optical modeling. It also provides a thorough analysis of the dynamic features of the designed glazing system. To preliminarily understand its potential energy impacts, this study implemented this newly designed dynamic glazing system into a comparative analysis and compared it relative to the baseline model with static standards-compliant windows (ASHRAE standard 90.1 2019). This was achieved via *EnergyPlus* EMS modeling and simulation. Because of the specific dynamic SHGC range attained in this system, the results show that this dynamic system is not practical for extremely hot climates. However, for mixed and slightly cold climates, the system could save building heating and cooling energy use by 15%–30%. Furthermore, the system did not significantly impact lighting energy use, showing that the system worked as transparent clear glass with no interruption in daylight transmission. Future work will focus on design optimization in terms of transition temperature settings, initial and ending temperature points for deflection, and solar optical properties of the static and dynamic strips to maximize energy savings.

Acknowledgements

This project is supported by the NSF award: # 2001207: CAREER: Understanding the Thermal and Optical Behaviors of the Near Infrared (NIR)-Selective Dynamic Glazing Structures.

Declaration of competing interest

The authors have no competing interests to declare that are relevant to the content of this article.

Ethical approval

This study does not contain any studies with human or animal subjects performed by any of the authors.

Author contribution statement

All authors contributed to the study conception and design. Design, modeling, simulation, and analysis were performed by Neda Ghaeili Ardabili and Julian Wang. The data collection and curation were completed by Yanxiao Feng. All authors commented on previous versions of the manuscript. All authors read and approved the final manuscript."

References

Abbasi Mahroo H, Vafamehr M (2023). Structural optimization of four designed roof modules: Inspired by Voronax grid shell structures. *Frontiers of Architectural Research*, 12: 129–147.

Aburas M, Soebarto V, Williamson T, et al. (2019). Thermochromic smart window technologies for building application: A review. *Applied Energy*, 255: 113522.

Aburas M, Ebendorff-Heidepriem H, Lei L, et al. (2021). Smart windows–Transmittance tuned thermochromic coatings for dynamic control of building performance. *Energy and Buildings*, 235: 110717.

Al-Masrani SM, Al-Obaidi KM (2019). Dynamic shading systems: A review of design parameters, platforms and evaluation strategies. *Automation in Construction*, 102: 195–216.

Atzeri AM, Gasparella A, Cappelletti F, et al. (2018). Comfort and energy performance analysis of different glazing systems coupled with three shading control strategies. *Science and Technology for the Built Environment*, 24: 545–558.

Barone G, Zacharopoulos A, Buonomano A, et al. (2022). Concentrating PhotoVoltaic glazing (CoPVG) system: modelling and simulation of smart building façade. *Energy*, 238: 121597.

Bui DK, Nguyen TN, Ghazlan A, et al. (2021). Biomimetic adaptive electrochromic windows for enhancing building energy efficiency. *Applied Energy*, 300: 117341.

Cedeno Laurent JG, Samuelson HW, Chen Y (2017). The impact of window opening and other occupant behavior on simulated energy performance in residence halls. *Building Simulation*, 10: 963–976.

Chel A, Kaushik G (2018). Renewable energy technologies for sustainable development of energy efficient building. *Alexandria Engineering Journal*, 57: 655–669.

Curcija DC, Zhu L, Czarnecki S, et al. (2015). Berkeley Lab WINDOW. Berkeley, CA, USA.

Dabbagh M, Krarti M (2021). Energy performance of switchable window insulated shades for US residential buildings. *Journal of Building Engineering*, 43: 102584.

de Vries SB, Loonen RCGM, Hensen JLM (2021). Multi-state vertical-blinds solar shading—Performance assessment and recommended development directions. *Journal of Building Engineering*, 40: 102743.

DeForest N, Shehabi A, Selkowitz S, et al. (2017). A comparative energy analysis of three electrochromic glazing technologies in commercial and residential buildings. *Applied Energy*, 192: 95–109.

Duan Q, Feng Y, Wang J (2021). Clustering of visible and infrared solar irradiance for solar architecture design and analysis. *Renewable Energy*, 165: 668–677.

Engineered Materials Solutions (n.d.). Thermostatic Bimetal Designer's Guide. Available at https://www.emsclad.com/fileadmin/Data/Divisions/EMS/Header/Bimetal_Desingers_Guide.pdf.

Furuto A (2012). Bloom/DO|SU Studio Architecture. Archdaily. Available at https://www.archdaily.com/215280/bloom-dosu-studio-architecture. Access 20 Aug 2022.

Hinkle L, Ardabili NG, Wang J (2022). Parametric simulation of dynamic glazing system with changeable NIR response. arXiv preprint arXiv: 2210.04876.

Ilbeigi M, Ghomeishi M, Dehghanbanadaki A (2020). Prediction and optimization of energy consumption in an office building using artificial neural network and a genetic algorithm. *Sustainable Cities and Society*, 61: 102325.

Jung W, Hong T, Oh J, et al. (2019). Development of a prototype for multi-function smart window by integrating photovoltaic blinds and ventilation system. *Building and Environment*, 149: 366–378.

Kang J, Liu J, Shi F, et al. (2022). Facile fabrication of VO_2/SiO_2 aerogel composite films with excellent thermochromic properties for smart windows. *Applied Surface Science*, 573: 151507.

Kunwar N, Cetin KS, Passe U, et al. (2019). Full-scale experimental testing of integrated dynamically-operated roller shades and lighting in perimeter office spaces. *Solar Energy*, 186: 17–28.

Le DM, Park DY, Baek J, et al. (2022). Multi-criteria decision making for adaptive façade optimal design in varied climates: energy, daylight, occupants' comfort, and outdoor view analysis. *Building and Environment*, 223: 109479.

Lei Q, Wang L, Xie H, et al. (2022). Active-passive dual-control smart window with thermochromic synergistic fluidic glass for building energy efficiency. *Building and Environment*, 222: 109407.

Li J, Duan Q, Zhang E, et al. (2018). Applications of shape memory polymers in kinetic buildings. *Advances in Materials Science and Engineering*, 2018: 7453698.

Li Z, Zhang S, Chang J, et al. (2020). Simulation study on light environment performance and heat gain of applying a bimetal automatic shading device to rooms. *Energy and Buildings*, 211: 109820.

Lin Q, Zhang Y, Mieghem AV, et al. (2020). Design and experiment of a sun-powered smart building envelope with automatic control. *Energy and Buildings*, 223: 110173.

Lobaccaro G, Wiberg AH, Ceci G, et al. (2018). Parametric design to minimize the embodied GHG emissions in a ZEB. *Energy and Buildings*, 167: 106–123.

Luo Z, Sun C, Dong Q (2020). A daylight-linked shading strategy for automated blinds based on model-based control and Radial Basis Function (RBF) optimization. *Building and Environment*, 177: 106854.

Montaser Koohsari A, Heidari S (2022). Subdivided venetian blind control strategies considering visual satisfaction of occupants, daylight metrics, and energy analyses. *Energy and Buildings*, 257: 111767.

Peres Suzano e Silva AC, Flora Calili R (2021). New building simulation method to measure the impact of window-integrated organic photovoltaic cells on energy demand. *Energy and Buildings*, 252: 111490.

Rizi RA, Eltaweel A (2021). A user detective adaptive facade towards improving visual and thermal comfort. *Journal of Building Engineering*, 33: 101554.

Shafaghat A, Keyvanfar A (2022). Dynamic façades design typologies, technologies, measurement techniques, and physical performances across thermal, optical, ventilation, and electricity generation outlooks. *Renewable and Sustainable Energy Reviews*, 167: 112647.

Sheikh WT, Asghar Q (2019). Adaptive biomimetic facades: Enhancing energy efficiency of highly glazed buildings. *Frontiers of Architectural Research*, 8: 319–331.

Shen L, Han Y (2022). Optimizing the modular adaptive façade control strategy in open office space using integer programming and surrogate modelling. *Energy and Buildings*, 254: 111546.

Soudian S, Berardi U (2021). Development of a performance-based design framework for multifunctional climate-responsive façades. *Energy and Buildings*, 231: 110589.

Sun Y, Liu X, Ming Y, et al. (2021). Energy and daylight performance of a smart window: Window integrated with thermotropic parallel slat-transparent insulation material. *Applied Energy*, 293: 116826.

Syed M, Moeini M, Okumus P, et al. (2021). Analytical study of tessellated structural-architectural reinforced concrete shear walls. *Engineering Structures*, 244: 112768.

Tcelykh LO, Kozhevnikova VY, Goloveshkin AS, et al. (2022). Sensing temperature with Tb-Eu-based luminescent thermometer: A novel approach to increase the sensitivity. *Sensors and Actuators A: Physical*, 345: 113787.

Wang J, Beltrán LO, Kim J (2012). From static to kinetic: A review of acclimated kinetic building envelopes. In: Proceedings of the World Renewable Energy Forum (WREF 2012), Denver, CO, USA.

Wang J, Beltrán L (2016). A method of energy simulation for dynamic building envelopes. In: Proceedings of IBPSA-USA SimBuild 2016, Salt Lake City, UT, USA.

Wang J, Caldas L, Chakraborty D, et al. (2016). Selection of energy efficient windows for hot climates using genetic algorithms optimization. In: Proceedings of PLEA. Los Angeles, CA, USA.

Wu H, Zhang T (2022). Optimal design of complex dynamic shadings: Towards sustainable built environment. *Sustainable Cities and Society*, 86: 104109.

Zhang J, Liu N, Wang S (2020). A parametric approach for performance optimization of residential building design in Beijing. *Building Simulation*, 13: 223–235.

Zhu D, Hong T, Yan D, et al. (2013). A detailed loads comparison of three building energy modeling programs: EnergyPlus, DeST and DOE-2.1E. *Building Simulation*, 6: 323–335.

View publication stats